Charge-Carrier Mobilities in Liquid Helium at the Vapor Pressure*

K. W. Schwarz
Department of Physics and The James Franck Institute, The University of Chicago, Chicago, Illinois 60637
(Received 15 November 1971)

Accurate values of the mobility of positive- and negative-charge carriers in liquid helium are presented. The measurements were carried out at the vapor pressure, over a temperature range of $0.27\,°K < T < 5.18\,°K$ for negative-charge and $0.37\,°K < T < 5.18\,°K$ for positive-charge carriers. A detailed description is given of the experimental techniques and of possible sources of error.

I. INTRODUCTION

Both the positive- and the negative-charge carriers in liquid helium consist of localized structures[1,2] which may be thought of roughly as charged spheres with radii of order 10 Å. Under the influence of an electric field, such a charge carrier will accelerate until the mean drag force F exerted by the liquid balances the applied electric force $e\mathcal{E}$. By measuring the average drift velocity v_D as a function of field one therefore obtains F as a function of v_D. At sufficiently low drift velocities, F is proportional to v_D, and results are conventionally given in terms of the mobility $\mu = v_D/\mathcal{E} = ev_D/F$.

If μ is known as a function of temperature one can obtain a great deal of information about the nature of the charge-carrier structures and the way in which they interact with the liquid. Below about 1.7 °K the density of the elementary excitations in the superfluid is low enough so that they interact independently with the charge. It has been shown by Baym *et al.*[3] that in this regime the transport theory takes a simple enough form to permit the calculation of μ from detailed microscopic models for the interaction between the charge carriers and the elementary excitations. Nearer to the λ point, viscous effects become important, and a theoretical treatment of this more complicated situation has not yet been attempted. Above T_λ liquid helium is a normal fluid, and μ may be calculated successfully in the hydrodynamic approximation.[4] As one approaches the critical point, the hydrodynamic approximation appears to break down because of critical-point fluctuations, and the problem again becomes complicated.

There are therefore a variety of interesting problems associated with trying to interpret the behavior of μ in the various temperature regions, and it is desirable to know this quantity accurately over a wide range of temperature. The purpose of this paper is to present the results of a series of experiments carried out with the aim of obtaining reliable values for the mobilities of positive- and negative-charge carriers in liquid helium. Some of the data have previously been published in preliminary form,[4-6] and their theoretical interpretation has been discussed in some detail. Here we shall concentrate on describing how the measurements were performed and on estimating their reliability. It is hoped that our values will prove of sufficient accuracy and extensiveness to serve as a useful benchmark for other workers in the field.

II. CYROGENICS AND TEMPERATURE MEASUREMENTS

Two different cryostats were used in the course of the experiments. A He^3 refrigerator for measurements at $T < 1.4$ °K and low electric fields is shown in Fig. 1(a). Our design is essentially an enlarged

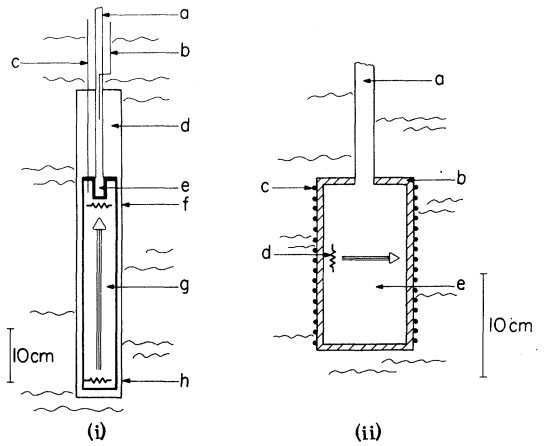

FIG. 1. (i) Schematic of He^3 refrigerator used for measurements below 1.4 °K, with (a) He^3 pump line, (b) He^3 return capillary, (c) He^4 condensing capillary, (d) vacuum space, (e) He^3 cup, (f) temperature-sensing resistor, (g) He^4 sample chamber, and (h) heater. The vertical arrow shows the location of the drift space. The refrigerator is immersed in a He^4 bath at 1.2 °K. (ii) Schematic of cryogenic apparatus used for measurements above 1.1 °K, with (a) He^4 vapor pressure calibration line, (b) thick copper wall, (c) heater, (d) temperature-sensing resistor, and (e) sample chamber. The horizontal arrow shows the location of the drift space. The sample chamber is surrounded by a He^4 bath at the working temperature.

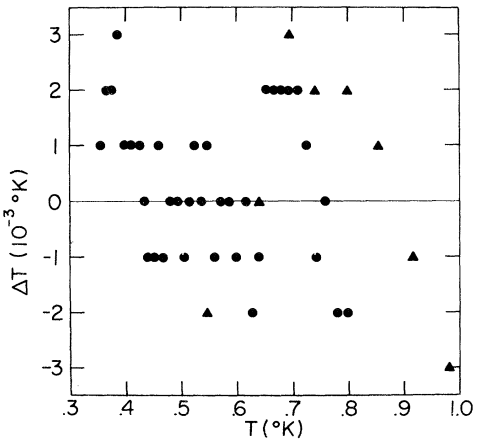

FIG. 2. Deviation of individual temperature-calibration points from a fitted curve of the form $\log_{10}P = A - B\log_{10}R$, with both ΔP and R expressed in terms of temperature. Points for $T < 0.48\,^{\circ}\mathrm{K}$ have been corrected for the thermomolecular effect. Circles are calibration points taken with the system drifting up in temperature, while points indicated by triangles were taken with the temperature regulated.

and improved version of that used by Reif and Meyer.[7] The He^4 sample chamber has a volume of about 1 liter, in order to accommodate a long drift space. The He^3 pump lines were also made large to improve the ultimate temperature of the refrigerator and to facilitate temperature calibrations against the He^3 vapor pressure. The lowest temperature attained with this system was $0.26\,^{\circ}\mathrm{K}$.

Since μ is a very strong function of temperature, it was necessary to measure and control the temperature as accurately as possible. The sensing element used to measure T in the He^3 range was a 470-Ω Speer carbon resistor,[8] "Epoxied" onto the bottom of the He^3 cup and in contact with the liquid He^4 in the sample chamber. This resistance was measured with an ac bridge,[9] designed to operate at low power levels to avoid erroneously high-temperature readings resulting from heating of the resistor. In practice, the driving oscillator signal was reduced until the measured resistance became independent of the power level. At $0.5\,^{\circ}\mathrm{K}$, this corresponded to a dissipation of less than 10^{-9} W. Temperature was kept constant by using the out of balance signal from the bridge to control a heater located near the bottom of the sample chamber. With proper setting of the He^3 pumping speed, the temperature was maintained constant to within $10^{-4}\,^{\circ}\mathrm{K}$ using a heater power of less than 3×10^{-5} W.

The carbon resistor was established as a secondary temperature standard by calibrating it against the He^3 vapor pressure.[10] The pressure was determined to an accuracy of about 2% by means of a CVC 100A McLeod gauge. This corresponds to an uncertainty of about $0.001\,^{\circ}\mathrm{K}$ in the individual calibration points. For $T \lesssim 0.53\,^{\circ}\mathrm{K}$, the vapor pressure was measured with the He^3 pump turned off and the sample chamber drifting upward in temperature. At higher T the pressure was measured both with temperature drifting and regulated. The measured dependence of the resistance on the vapor pressure was well represented by an expression[11] of the form $\log_{10}P = A - B\log_{10}R$, where for our particular resistor $A \approx 25.25$, $B \approx 6.45$ if P is measured in μ Hg and R in Ω. Since A and B would usually shift by a fraction of a percent when the system was warmed to room temperature and cooled down again, it was necessary to recalibrate the resistor for each run. In Fig. 2 we show a typical calibration in terms of the deviations of the individual calibration points from the fitted functional form given above. ΔP is expressed in terms of the equivalent ΔT to the nearest millidegree, and R is given in terms of the equivalent T. Only points above $T = 0.48\,^{\circ}\mathrm{K}$ were used to determine A and B. Below this temperature, the measured P was corrected for the thermomolecular effect according to the work of Roberts and Sydoriak.[12] The actual correction was calculated from our He^3-pump-line geometry, and varied from $0.001\,^{\circ}\mathrm{K}$ at $T = 0.48\,^{\circ}\mathrm{K}$ to $0.016\,^{\circ}\mathrm{K}$ at $T = 0.36\,^{\circ}\mathrm{K}$, our lowest calibration point. From Fig. 2 one sees that in the region above $T = 0.48\,^{\circ}\mathrm{K}$, where the thermomolecular effect is unimportant, the individual calibration points are in excellent agreement with the fitted relation $\log_{10}P = A - B\log_{10}R$. Below this temperature, the agreement is equally good after the proper correction has been made for the thermomolecular effect. All individual calibration points lie within $0.003\,^{\circ}\mathrm{K}$ of the fitted curve, and the standard deviation is about $0.001\,^{\circ}\mathrm{K}$, consistent with the inaccuracy in measuring the He^3 vapor pressure.

One possible source of error in the calibration procedure is the existence of a systematic temperature difference between the liquid He^3 in the cup and the He^4 in the sample chamber, arising from the Kapitza thermal-boundary resistance.[13] The total area across which heat was exchanged from sampling to cooling chamber was about 100 cm^2, and the maximum heat leak across this area was estimated to be 10^3 erg sec^{-1} by measuring the rate at which the He^3 was pumped out of the cooling chamber when the He^3-return capillary was shut off. From the work of Anderson *et al.*,[14] one can therefore conclude that any temperature error introduced by the Kapitza resistance is less than $0.001\,^{\circ}\mathrm{K}$ across the whole calibration range. Combining this with the typical scatter of our calibrations shown in Fig. 2, we estimate the deviation of our secondary-temperature calibration from the 1962 He^3 vapor pressure scale to be of order $0.002\,^{\circ}\mathrm{K}$.

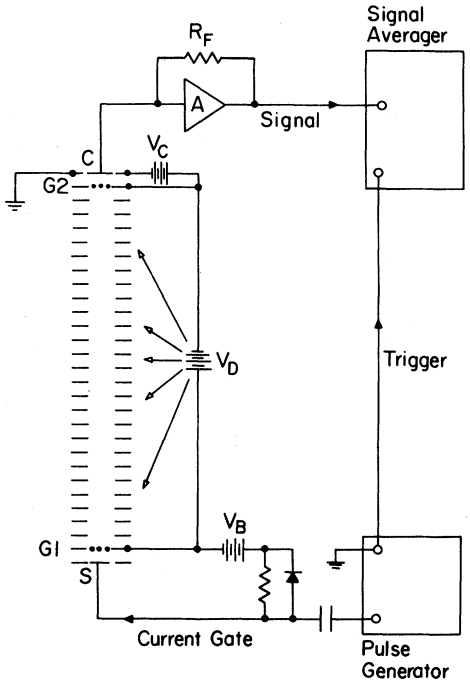

FIG. 3. Schematic of the low-temperature mobility cell and the associated electronics. The arrows denote V_D is divided evenly between the guard rings.

The accuracy of the absolute temperature measured by the carbon resistor is therefore limited by the accuracy of the 1962 He^3 scale, which may contain errors as large as 0.003 °K.

For $T > 1.1$ °K, the mobilities become rather small, and it is desirable to have a short drift space to which high fields can be applied. Measurements for $1.1\,°K < T < 5.2\,°K$ were therefore carried out in the system shown in Fig. 1(b). The sample chamber consisted of a copper can with walls $\frac{1}{4}$ in. thick, immersed in the He^4 bath. Temperature was again controlled with an ac bridge, the sensing element being a 20-Ω Allen-Bradley resistor placed inside the sample chamber at the level of the drift space. The controlling heater consisted of a wire wound uniformly around the copper can, the point of this arrangement being to provide an isothermal enclosure in order to minimize the thermal gradients that can occur in the normal-fluid regime.

The temperature in the sample chamber was determined from the He^4 vapor pressure,[15] measured with a Texas Instruments 145 quartz Bourdon tube gauge. Below the λ point, thermal gradients are negligible and this straightforward method yields results accurate to ~0.001 °K. To check on the importance of residual thermal gradients above the λ point, the temperature-sensing resistor was calibrated against He^4 vapor pressure in the region below the λ point. The result could again be satisfactorily fitted by an equation of the form $\log_{10}P = A - B\log_{10}R$. The resulting equation was then used to determine T above the λ point from the measured R. The maximum difference between the temperature determined by this method and that derived directly from the vapor pressure was ±0.02 °K over the range $T_\lambda < T < T_c$. We therefore take this as our uncertainty above the λ point.

III. METHOD OF MEASUREMENT

The measurements of drift velocity v_D versus field were carried out by directly observing the propagation of a pulse of charge carriers across the drift space. At low T, this was done by means of the apparatus schematized in Fig. 3. Charge carriers are produced in the liquid through the ionizing action of a 10-μC Am^{241} α-particle source S. A bias voltage V_B between S and the source grid $G1$ picks out one sign of charge carrier and injects it into the drift region, resulting in a current density in the range 10^{-13} to 10^{-12} A cm^{-2}. The drift space voltage V_D is divided by a network of 0.1% precision resistors, and applied to 25 equally spaced guard rings. According to numerical calculations, this arrangement keeps the drift space field uniform to ~$\frac{1}{4}$% over the path of the charge carriers. At the end of the drift space, the charge carriers pass through the guard grid $G2$ and are collected at C.

The cell used for measurements above 1.1 °K was very similar to the low-temperature cell shown in Fig. 3. The major difference was in the length: for the low-T system $S - G1 = 1.04$ cm, $G1 - G2 = 27.13$ cm, and $G2 - C = 1.04$ cm, while the short cell used at higher T had $S - G1 = 0.21$ cm, $G1 - G2 = 1.88$ cm, $G2 - C = 0.11$ cm. Five guard rings were used to maintain a uniform drift space field. Whereas the low-temperature cell was never used at drift space fields higher than 15 V cm^{-1}, the high-temperature system was designed to allow fields of up to 2500 V cm^{-1}.

Our method of measuring v_D was to gate the current ON or OFF by applying an additional voltage pulse across the $S - G1$ region. The resulting ON or OFF current pulse then propagates across the drift space with the characteristic drift velocity v_D. The current received at C is detected as a function of time by a fast electrometer consisting of a Philbrick P25 AH operational amplifier,[16] the output of which is fed into a RIDL 34-12B 400-channel analyzer run in the time-sweep mode. The time sweep is initiated by the $S - G1$ gating pulse, so that the corresponding signal is recorded on the analyzer with a delay equal to the time required for the charge carriers to cross the drift space. Since the current-noise level in the amplifier is of order 10^{-12} A, it is necessary to average over many events to obtain a good signal-to-noise ratio. In practice a repetitive gat-

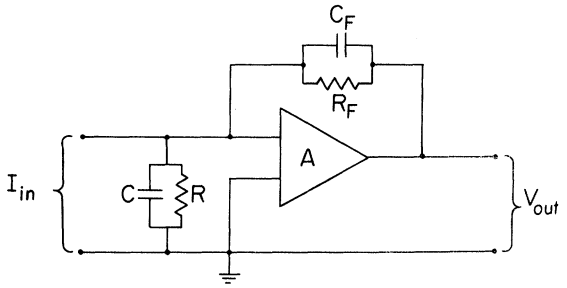

FIG. 4. Schematic of the fast electrometer used in the experiment, showing the main factors influencing its response.

ing pulse produced by a Tektronix 161 pulse generator is superimposed on the $S-G1$ bias voltage by means of the diode clamp shown in Fig. 3, each pulse triggering a new sweep of the analyzer.

An important consideration in interpreting the results obtained by this method is the accuracy with which the electrometer reproduces the time dependence of the current collected at C. The configuration in Fig. 4 shows the main sources of nonideal behavior. The frequency-dependent gain of an operational amplifier is to a good approximation given by $A(f) = if_0/f$ at frequencies above the low-frequency break point. The response of the electrometer to an idealized-step-function input-current pulse of amplitude I_0 can then easily be found:

$$V_{out} = -I_0 R_F \left[1 - e^{-At/2}\left(\cos\alpha t + \frac{A}{2\alpha}\sin\alpha t\right)\right], \quad (1)$$

where

$$A = \frac{R^{-1} + R_F^{-1} + 2\pi f_0 C_F}{C + C_F} \quad (2)$$

and

$$\alpha = \left(\frac{2\pi f_0}{R_F(C + C_F)} - \frac{A^2}{4}\right)^{1/2}. \quad (3)$$

The condition for critical damping is $\alpha = 0$, in which case the transfer function reduces to

$$V_{out} = -I_0 R_F[1 - e^{-At/2}(1 + \tfrac{1}{2}At)]. \quad (4)$$

Given R, C, and the unit-gain frequency f_0 of the amplifier, the rise time $\tau_{el} = 2/A$ at critical damping may be optimized by adjusting R_F and C_F. One constraint on these two quantities is given by the condition of critical damping, while a second is provided by requiring that $I_0 R_F$ be greater than the voltage-noise level of the amplifier, and not much less than the current noise times R_F. Thus there is a practical lower limit to the rise time. In our case, this turned out to be $\tau_{el} \sim 80$ μsec for the system designed to operate at He^3 temperatures, and $\tau_{el} \sim 15$ μsec for the higher-temperature system where more care was taken to minimize the input capacity. The calculated response was checked experimentally by applying a triangular-wave voltage to $G2$. This grid has a few pF capacitive coupling to the collector, resulting in a collector current proportional to the differentiated triangular wave. It is easy in this way to generate a square-wave collector current of amplitude 10^{-12} A, and to measure the response directly. The observed behavior was always in good agreement with predictions based on Eqs. (1)–(4).

To complete the discussion of the electrometry, we show in Fig. 5 the expected output of the critically damped electrometer with rise time τ_{el} when an idealized incoming current pulse arrives at the collector after a time of flight t_D. Note that after the pulse has arrived, there is a short interval when the signal increases as $(t - t_D)^2$, followed by a "leading edge" linear in time, and finally saturation to $-I_0 R_F$. In the real system, the $(t - t_D)^2$ tail will often be hidden in the noise, and the best way to determine t_D is to find the intercept of the leading edge with the base line. This must then be corrected for the "tail" by subtracting $0.25\tau_{el}$.

IV. EXPERIMENTAL DETAILS

Under actual running conditions the signal-averaged pulse read off the analyzer looked like Fig. 6 (a). The time of flight t_D of the charge carriers is short enough in this example so that the pulse shape is dominated by the electrometer response, and indeed in such a case one finds that the pulse shape is essentially that predicted in Fig. 5. An example of a pulse where the electrometer rise time is very short compared with the time of flight is given in Fig. 6(b). One sees that the leading edge is not a step function, but retains a certain intrinsic rise time. This may be explained by noting that the $G2 - C$ region forms a kind of Faraday cage, in that the collector begins to see an induced current the

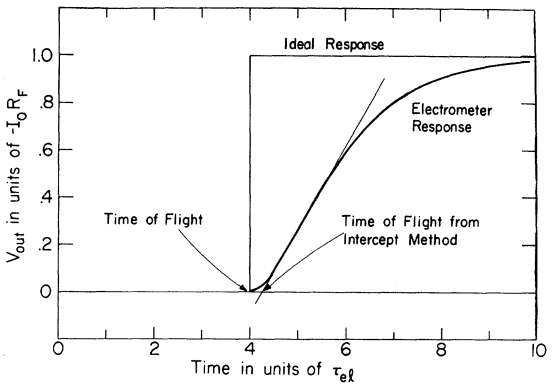

FIG. 5. Calculated response of the critically damped electrometer to a step function input current.

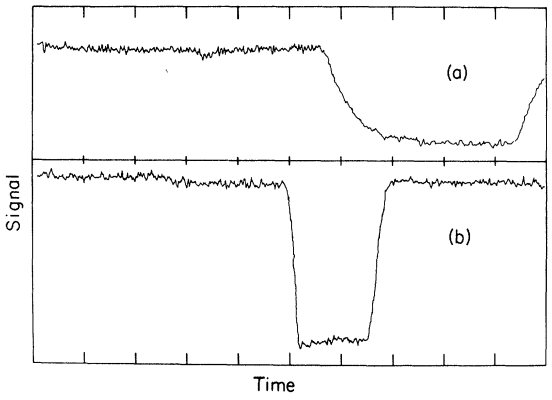

FIG. 6. Typical observed signals. In case (a) the shape of the pulse edge is dominated by the electrometer rise time; in case (b) it is dominated by the intrinsic rise time due to the geometry of the $G2-C$ region.

instant that the front edge of the current pulse passes $G2$. The collector current will rise as the pulse edge approaches the collector, in a manner which depends on the geometry of the $G2-C$ region only. If the field in the $G2-C$ region is kept the same as the drift space field, the intrinsic rise time should always be a constant fraction of t_D of order $l(G2-C)/l(G1-G2)\approx 2$ to 3%. This is consistent with our observations.

Over the entire range of T, $\mathcal{E}$, and v_D investigated by us, the observed shapes of the pulse edges could consistently be interpreted as arising from a combination of the intrinsic rise time and the response of the electrometer. No convincing evidence of any real smearing out of the edges of the actual current pulse due to nonuniform electric fields, grid effects, diffusion, or other causes was ever observed. That is, the current pulse propagates across the drift space without significantly changing in shape, and initiates an observed signal when it starts to cross $G2$. The time of flight determined as in Fig. 5 is then a true measure of the time taken by a charge carrier to cross the drift space and arrive at $G2$. We find that t_D measured in this way is independent of V_c, as expected if the effective collector position is at $G2$.

A possible source of error in t_D determined as above is space-charge spreading of the pulse, an effect which would not necessarily affect the shape of the pulse edges. This can easily be detected experimentally by looking at the length of the received pulse. At high signal levels or at very low drift velocities, space-charge effects indeed introduced significant errors in t_D. Care was therefore taken to avoid these conditions.

Several problems arose at very low temperatures. As the temperature is reduced, the mobility increases rapidly. In order to make measurements in the region where v_D is proportional to $\mathcal{E}$, one must therefore go to smaller drift space fields as the temperature is lowered. This is especially true of the positive carriers which have a much higher mobility than negatives below $T\sim 0.6\,^{\circ}\mathrm{K}$, and which in addition depart from linearity at lower drift velocities than the negatives. When a dc electrometer is hooked up to the collector and the current passing the cell is measured as a function of $\mathcal{E}_D$, the typical response is as shown in Fig. 7, curve (a). Here both the $S-G1$ field and the $G2-C$ field are kept constant at fairly high values. The tendency for the current to increase slowly with $\mathcal{E}_D$ at large fields results from the increased number of field lines from the source which penetrate into the drift space rather than terminating on $G1$. The low-field cutoff in curve (a) seems to arise from free charge which accumulates near $G2$ and produces a local repulsive field. Only if $\mathcal{E}_D$ is sufficient to override the local field will current pass through the cell. Once it was realized that the cutoff field was due to a charge layer near $G2$, several tricks were devised to reduce its importance, allowing us to work at lower $\mathcal{E}_D$. The first of these was to shoot in charge carriers of the opposite sign for a period of time in order to neutralize the charge layer. This would usually result in an improved curve (b). Increasing the collector field to a higher value might improve the performance somewhat further. The most effective trick, however, was to apply a large voltage between the first guard ring in front of $G2$ and the collector. This apparently had the double effect of focusing the incident beam, and of providing many more field lines passing through $G2$. It generally resulted in a greatly improved curve such as (c). The use of a focusing field before $G2$ of course distorts the field in the

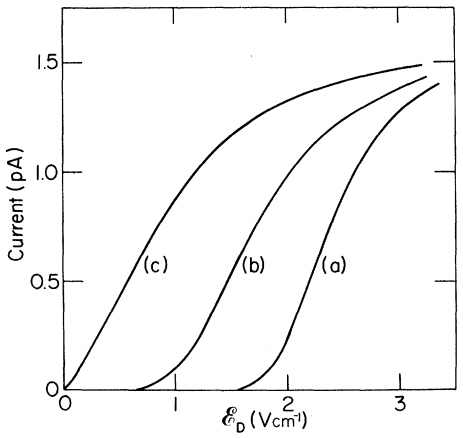

FIG. 7. dc current across the long cell as a function of drift space field. The curves are discussed in the text.

drift space and was therefore used only as a last resort. However, because of the great length of our low-T drift space and the close spacing of our guard rings, the distortion in $\mathcal{E}_D$ is confined to a region quite close to $G2$. The actual error introduced by a focusing field depends only on the ratio of the focusing field to the drift space field, and the necessary corrections were experimentally determined at higher temperatures by comparing t_D measured with and without focusing fields. Remaining uncertainties in this correction introduce errors of $\sim \pm 1\%$ in our final results. Using all of these various tricks, we were able to see signals propagating across the cell at fields as low as 0.030 V cm^{-1}, and were thus able to measure μ to much lower temperatures than previous workers.

One final problem which arose for the positive carriers at low T was due to the nucleation of quantized vortex rings by the source.[17] The $S-G1$ region is 1 cm long in our setup, and at $T > 0.45\,^\circ$K the energy-loss rate of the quantized rings is great enough so that they decay before they leave this region. An OFF voltage pulse then cuts the current of normal carriers off at $G1$, and gives the correct t_D. At lower T, however, the rings penetrate some distances into the drift space and then decay, resulting in an abnormally long t_D. This effect can readily be identified by noting that when the charge carriers enter the drift space as rings, t_D increases as the forward bias V_D is increased.

The problems presented by the source-nucleated rings were handled as follows: The $S-G1$ region was subjected to a weak back bias sufficient to make the vortex rings decay in the $S-G1$ region, but not strong enough to cause rapid collection of the resulting normal charge carriers. An ON voltage pulse then produces signals like those in Fig. 8, consisting of a small pulse corresponding to those carriers which had decayed and lost their rings and were hence suitable for our measurements plus a large and slower pulse of carriers which started out as quantized vortex rings. This interpretation is unambiguously verified by data such as those given in Figs. 8(a)–8(d), which show the slowing down of the ring pulse as the ON voltage is increased. One may also note from Fig. 8 the interesting fact that the ring pulse is quite sharply defined, indicating that all of the positive-charge carriers start out attached to quantized vortex rings of nearly the same energy.

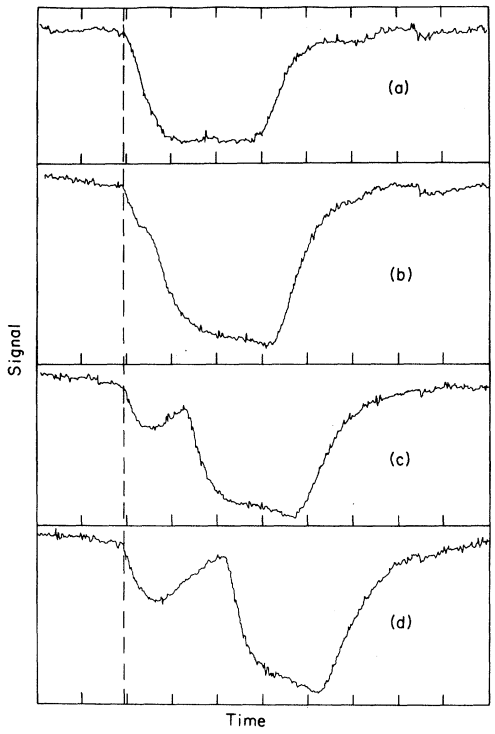

FIG. 8. Typical signals observed for an ON pulse of positive-charge carriers. The drift space field is kept constant, while the size of the ON field in the $S-G1$ region is progressively increased in curves (a)—(d). The traces clearly show the existence of a small pulse of normal carriers arising from source-nucleated quantized vortex rings which have been allowed to decay in the source region plus a large pulse of carriers coming directly from the source which enter the drift space as quantized vortex rings.

V. ANALYSIS AND RESULTS

The time of flight t_D is determined from the raw data in the manner discussed in Secs. III and IV. It is corrected for (a) the electrometer response; (b) time taken to cross $S-G1$, if an ON pulse is used; and (c) distortion from the focusing field, if one is used. The total correction to t_D never exceeded 5% in our experiment. For the long cell the effective length of the drift space is taken to be the distance $G1-G2$, with an estimated accuracy of $\frac{1}{2}\%$. The effective length of the short cell was determined by comparing measurements taken with both cells in the temperature region from 1.1–1.4 °K. It was found to be 3% shorter than the nominal geometrical length of 1.88 cm. The drift velocity v_D is then taken to be the effective length of the drift space divided by the corrected time of flight.

To determine μ at a given T, v_D was measured for several values of $\mathcal{E}$. Under good conditions and provided v_D was small enough, v_D vs $\mathcal{E}$ gave a straight line extrapolating through zero. At fields approaching the cutoff field, one would generally find abnormally low drift velocities, in agreement with the idea that the drift field is reduced by free charge in some region of the drift space. Using the various special tricks outlined in Sec. IV, we had no difficulty in obtaining good linear v_D-vs-$\mathcal{E}$ plots down to 0.27 °K for negatives and 0.55 °K for

TABLE I. Mobilities of charge carriers in He^4.

T (°K)	μ_- ($cm^2 V^{-1} sec^{-1}$)	μ_+ ($cm^2 V^{-1} sec^{-1}$)
0.274	1350	
0.283	1230	
0.291	1120	
0.300	1020	
0.310	925	
0.320	835	
0.332	750	
0.344	670	
0.357	605	
0.371	540	51900
0.378		47200
0.386	480	41800
0.394		38000
0.405	423	33600
0.411		29500
0.420	372	26300
0.429		23800
0.439	327	20500
0.450		17500
0.461	284	14600
0.472		12300
0.484	245	10100
0.498	225	8050
0.510	209	6420
0.526	190	4860
0.540	174	3730
0.555	156	2760
0.573	141	1980
0.590	125	1410
0.610	109	965
0.631	92.9	660
0.653	78.6	445
0.676	65.0	297
0.701	52.5	203
0.727	41.1	138
0.757	30.9	88.6
0.786	23.5	60.5
0.820	17.1	40.1
0.859	11.9	25.8
0.897	8.40	17.4
0.945	5.63	11.10
0.996	3.77	7.15
1.048	2.60	4.80
1.132	1.51	2.57
1.196	1.00	1.66
1.297	0.576	0.916
1.398	0.360	0.548
1.500	0.242	0.353
1.602	0.174	0.244
1.708	0.133	0.180
1.812	0.105	0.139
1.913	0.0842	0.109
2.016	0.0647	0.0842
2.117	0.0461	0.0622
2.132	0.0437	0.0586
2.147	0.0405	0.0555
2.163	0.0368	0.0517
2.169	0.0356	0.0504
2.174	0.0346	0.0496
2.20	0.0326	0.0472
2.26	0.0301	0.0452
2.37	0.0278	0.0430
2.49	0.0261	0.0420
2.64	0.0247	0.0413
2.82	0.0234	0.0412
3.02	0.0226	0.0416
3.25	0.0218	0.0423
3.50	0.0211	0.0435
3.77	0.0203	0.0449
3.93	0.0201	0.0460
4.16	0.0196	0.0470
4.33	0.0191	0.0480
4.45	0.0187	0.0487
4.55	0.0186	0.0498
4.70	0.0180	0.0497
4.84	0.0176	0.0492
4.96	0.0172	0.0489
5.01	0.0169	0.0483
5.05	0.0167	0.0473
5.08	0.0165	0.0462
5.12	0.0161	0.0447
5.16	0.0158	0.0401
5.18	0.0157	0.0376

positives. The few plots for which not all points lay within ± 1% of a straight line extrapolating through zero were rejected.

For positive carriers below 0.55 °K, the measured v_D was above the linear regime even at the lowest $\mathcal{E}$ for which a signal could be seen. To determine μ_+, it was necessary to extrapolate v_D versus $\mathcal{E}$ down into the linear region. This can be done with some confidence, since v_D ($\mu\mathcal{E}$) varies only slowly with temperature. The shape of the v_D ($\mu\mathcal{E}$) curve was determined at 0.590 °K by direct measurement, and then used for extrapolating the lower-temperature results. This procedure gave unambiguous results down to 0.45 °K, in the sense that v_D ($\mu\mathcal{E}$) did not appear to change significantly as the temperature was lowered. Below 0.45 °K there is some evidence that v_D ($\mu\mathcal{E}$) begins to change, perhaps because He^3 impurity scattering becomes important. By comparing points adjacent in temperature, one can push the results to somewhat lower temperatures still, but the estimated errors increase rapidly.

Our final values for μ_+ and μ_- are given in Table I. As discussed earlier, the estimated deviation of our temperature scale from the 1962 He^3 and the 1958 He^4 standards is of order 0.002 °K below the λ point and of order 0.02 °K above. The absolute error in our values of μ is conservatively estimated as ± 2%. This includes the uncertainty in the various corrections discussed earlier as well as random variations of order 1% which were found when a given measurement was repeated after several

months. Because of the extrapolation necessary at low temperatures, the estimated uncertainties in μ_+ increase smoothly from ± 2% at 0.439 °K to ± 10% at 0.371 °K. It should be noted that the 2% uncertainty in μ is roughly consistent with the probable error in the absolute temperature.

A number of other workers have previously measured μ_+ and μ_- over various more limited temperature ranges.[18–22] Their results are generally in reasonable agreement with those of Table I. The only values which are expected to be of an accuracy comparable to ours are those obtained by Brody in the range $1.25\,^{\circ}\mathrm{K} \leq T \leq 2.2\,^{\circ}\mathrm{K}$ by a method very similar to our own. Although Brody conservatively quotes an error of ± 5% for his values, the agreement with our data is actually better than 2% for all of his points.

ACKNOWLEDGMENTS

I wish particularly to thank Professor R. W. Start for his generous support and his active interest in this work. Thanks are also due to R. M. Ostermeier, who took most of the data above 1 °K. Finally, I wish to acknowledge the many useful and pleasant discussions I have had with the late Professor L. Meyer, who was a pioneer in this field as in so many others.

---

*Work supported in part by the Advanced Research Projects Agency and in part by the U. S. Army Research Office (Durham).

[1]K. R. Atkins, Phys. Rev. 116, 1339 (1959).

[2]C. G. Kuper, Phys. Rev. 122, 1007 (1961).

[3]G. Baym, R. G. Barrera, and C. J. Pethick, Phys. Rev. Letters 22, 20 (1969).

[4]R. M. Ostermeier and K. W. Schwarz (unpublished).

[5]K. W. Schwarz and R. W. Stark, Phys. Rev. Letters 21, 967 (1968).

[6]K. W. Schwarz and R. W. Stark, Phys. Rev. Letters 22, 1278 (1969).

[7]F. Reif and L. Meyer, Phys. Rev. 119, 1164 (1960).

[8]W. C. Black, Jr., W. R. Roach, and J. C. Wheatley, Rev. Sci. Instr. 35, 587 (1964).

[9]This bridge, designed by D. Zimmerman, is similar to that of C. Blake, C. E. Chase, and E. Maxwell [Rev. Sci. Instr. 29, 715 (1958)].

[10]T. R. Roberts, R. H. Sherman, and S. G. Sydoriak, in *Progress in Low Temperature Physics*, edited by C. J. Gorter (North-Holland, Amsterdam, 1964), Vol. IV, p. 480.

[11]S. Cunsolo, M. Santini, and M. Vincentini-Missoni, Cryogenics 5, 168 (1965).

[12]T. R. Roberts and S. G. Sydoriak, Phys. Rev. 102, 304 (1956).

[13]P. L. Kapitza, J. Phys. (USSR) 4, 181 (1941).

[14]A. C. Anderson, J. I. Connolly, and J. C. Wheatley, Phys. Rev. 135, 910 (1964).

[15]F. G. Brickwedde, H. van Dijk, M. Durieux, J. R. Clement, and J. K. Logan, J. Res. Natl. Bur. Std. (U. S.) 64A, 1 (1960).

[16]W. H. Wing and T. M. Sanders, Rev. Sci. Instr. 38, 1341 (1967).

[17]G. W. Rayfield, Phys. Rev. 168, 222 (1967).

[18]See Ref. 7.

[19]L. Meyer, H. T. Davis, S. A. Rice, and R. J. Donnelly, Phys. Rev. 126, 1927 (1962).

[20]A. Dahm, J. Levine, J. Penley, and T. M. Sanders, Jr., in *Proceedings of the Seventh International Conference on Low-Temperature Physics, Toronto*, 1960, edited by G. M. Graham and A. C. Hollis-Hallet (University of Toronto Press, Toronto, Canada, 1961), p. 495.

[21]M. Kuchnir, Ph. D. thesis (University of Illinois, 1966) (unpublished).

[22]B. A. Brody, Ph. D. thesis (University of Michigan, 1970) (unpublished).